Super-High-Speed Lightwave Demodulation using the Nonlinearities of an Avalanche Photodiode

Young-Kyu Choi

Abstract - Even though the modulating signal frequency of the light is too high to detect directly, the signal can be extracted by frequency conversion at the same time as the detection by means of the non-linearity of the APD. An analysis is presented for super-high-speed optical demodulation by an APD with electronic mixing. A normalized gain is defined to evaluate the performance of the frequency conversion demodulation. The nonlinear effect of the internal capacitance was included in the small signal circuit analysis. We showed theoretically and experimentally that the normalized gain is dependent on the down converted difference frequency component. In the experiment, the down converted different frequency outputs became larger than the directly detected original signal for the applied local signal of 20dBm.

Keywords : photodiode, APD, optical mixing, lightwave deodulation, frequency conversion

1. Introduction

As the lightwave modulation speed has been increased, high-speed photodiodes and high-sensitivity optical receivers have been closed up as the vital components in the lightwave communication systems. Recently, p-i-n photodiodes operating at up 110 GHz and also APD's operating at several tens of GHz have been developed [1-3]. However, because these photodiodes are composed of the semiconductor p-n junction, their operating speed is limited. In order to overcome such limitations, superlattice or waveguide- type photodiodes have been intensively studied[4-5].

Even though the lightwave is modulated with the high-frequency signal beyond the 3dB cutoff frequency range of the photodiode, the photons of the high-frequency components should be generated inside the photodiodes. However, because of bypass by the internal capacitance, these photons could not come out as the output photo-current.

As a way to transcend the limitations, and to realize super-high-speed lightwave demodulation, optical mixing demodulation utilizing the nonlinearities of the photodiode were developed. In these cases, the photodiodes are used simultaneously as a photo-detector and an electronic frequency conversion mixer. This concept was first proposed by Davis and Kulczyk[6-7]. They used the nonlinearity of the multiplication factor of the APD for frequency conversion, and demonstrated improvement of the SNR. Seeds and Lenoir developed a more general multiplication model of the APD, and discussed the conversion loss and noise properties[8-9]. However, all of the previous reports deal with the lower frequency below the 3dB cutoff frequency region. In other words, the previous works were only focused on the detectable frequency bandwidth of the photodiode so that the results were consistently concerned with the conversion loss. The frequency characteristics of the optical mixing demodulation are not taken into account. If this method is extended to a higher frequency region beyond the cutoff, we might take advantage of the merits of the method in the super-high-speed light wave communication system.

In this paper, we have theoretically analyzed the frequency conversion demodulation method. In addition, qualitative experiments are carried out to confirm the theoretical analysis. We also have presented a small signal analysis for super-high-speed photo-detection using an APD as both the photodetector and the electronic mixer. In chapter 2 and 3, we have revealed the physical background and showed the basic theory of this method, respectively. We estimated the normalized gain of the method for the practical circuit parameters in chapter 4. The fundamental experiments were carried out in chapter 5, and the experimental results were discussed in chapter 6. We have summarized the conclusions in chapter 7.

Manuscript received: Sep. 19, 2002, accepted: Oct. 14, 2002
Young-Kyu Choi is with the Department of Photonics, Faculty of Engineering, Silla University Busan, 617-736 Korea.

2. Physical background

A high-speed APD has a configuration in which the light absorption region and the multiplication region are separated. A general APD model is shown in Fig. 1. The electron-hole pairs to be generated by light absorption are separated by a high electric-field applied to the depletion region, so that the holes and the electrons are diverted to the p-region and the n-region, respectively. The high energy holes accelerated by a high electric-field enter into the multiplication region, and they generate new electron- hole pairs.

When the carriers are generated by light in the absorption region, the drift velocity and the avalanche multiplication factor change non-linearly depending on the intensity of the bias-voltage. While the electron-hole pairs flow as the photo current inside the photodiode, the general currrent-voltage characteristics of the diode are exhibited. Further, the width of the depletion region and the internal capacitance vary nonlinearly by the bias- voltage. The photodiode characteristics related with the bias-voltage are listed in Table 1[10-11]. Here, V is the voltage applied to the diode, and E is the resultant electric-field. These characteristics will totally affect the output of the optical signal and the frequency response of the photodiode.

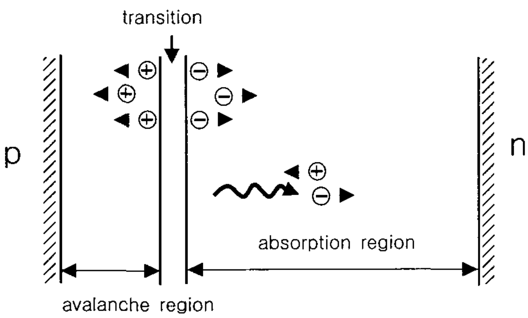

Fig. 1 Schematic cross-section of an APD

If the bias-voltage of an APD is modulated by the local signal at the same time as the photo detection, the optical signal and the local oscillator signal are mixed in the APD so that electronic frequency mixing takes place. In this case, if the sub-carrier multiplexing method is used, the original base-band signal is contained either in the frequency or in the phase of the sub-carrier as seen in Eq. (7) hereafter [12]. Therefore, the base-band signal can be extracted without distortion as the difference frequency component converted toward a lower frequency [13]. Among the many non- linearities of the APD, we have chosen the multiplication factor(M) for the electronic mixing parameter.

Table 1 APD characteristics dependent on bias voltage

drift velocity	$v_p = \mu_n E, \quad v_p = \mu_p E$
internal capacitance	$C = C_o(1 - v/V_D)^{\,n} \ \left(n = \frac{1}{2} \sim \frac{1}{3}\right)$
width of depletion layer	$\phi = \phi_o(V_D - V)^n \ \left(n = \frac{1}{2} \sim \frac{1}{3}\right)$
Multiplication factor	$M = 1/\{1 - (v/V_B)^n \ (n = 3 \sim 6)$
diode I-V characteristic	$I = I_s(e^{qv/kT} - 1)$

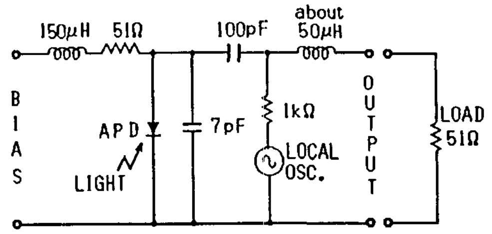

Fig. 2 Fabricated demodulation circuit

3. Basic theory of electronic mixing demodulation

The light demodulation circuit used for the experiment is shown in Fig. 2. Let us consider the case in which an APD is used. When the light intensity is modulated with the signal of the sub-carrier frequency f_s, the modulation index of $|m|$, and the phase $\theta(t)$, the light is

$$P(t) = P_o\,[1 + |m|\cos\{2\pi f_s t + \theta(t)\}], \tag{1}$$

where P_o is the dc light power. When the light is fed to the APD, then a photo-current flow in the APD is

$$I_p(t) = M(v)\eta' P_o[1 + |m|\cos\{2\pi f_s t + \theta(t)\}] \tag{2}$$

where $M(v)$ is the multiplication factor of the APD given by

$$\eta' = (e/h\nu)\eta_p\eta_c\ . \tag{3}$$

Here, η' is the effective efficiency of the photo detector, η_p is the efficiency in the particle state quantum efficiency), and η_c is the efficiency of the electronic circuit(electrical circuit efficiency). If the bias voltage of the APD is modulated by the local oscillator signal of V_l at the frequency of f_{lo}, then

$$v(t) = V_b + V_l\cos 2\pi f_{lo}t\ . \tag{4}$$

Since the multiplication factor $M(v)$ is empirically given in terms of the bias voltage as

$$M(v) = \frac{1}{1 - \left(\frac{v(t)}{V_B}\right)^n} \quad (n = 3 \sim 6)\ , \tag{5}$$

then substitution of (4) into (5), and expansion in a Taylor series near V_b give

$$M = M(V_b) + M'(V_b)V_l\cos 2\pi f_{lo}t + \cdots\ , \tag{6}$$

where $M' = dM/dV$. When Eq. (6) is substituted into Eq. (2), the photo current is

$$I_p(t) = M(V_b)P_o\eta'[1+|m|\cos\left\{2\pi f_s t+\theta(t)+\frac{M'(V_b)}{M(V_b)}V_l\cos 2\pi f_{lo}t\right. + \frac{1}{2}|m|\frac{M'(V_b)}{M(V_b)}V_l\cos 2\pi\{(f_s-f_{lo})+\theta(t)\}+\cdots] \tag{7}$$

In addition to the signal frequency f_s, the up-and down-converted frequency components $f_{\pm}=f_s \pm f_{lo}$ also appear. Usually, the detected optical signal current is bypassed by the internal capacitance between the APD terminals so that the apparent quantum efficiency is decreased as the signal frequency is increased. Hence, η_c can be expressed as a function of frequency such as $\eta_c(f_s)$ or $\eta_c(f_-)$. The ratio of the magnitude of the f_- component to the f_s component can be written as

$$G=\left|\frac{M'(V_b)V_l}{2M(V_b)}\right|\frac{\eta_c(f_-)}{\eta_c(f_s)}. \tag{8}$$

If the dc bias V_b is set near breakdown voltage V_B, $|M'(V_b)V_l/2M(V_b)|$ in (8) increases without limits. On the other hand, if a local oscillator signal f_{lo} is chosen such that $f_-=(f_s-f_{lo})$ is sufficiently small, the electric circuit efficiency $\eta_c(f_-)$ become a constant value of $\eta_c(0)=1$. Hence, if the modulation frequency f_s is much higher than the bandwidth of the APD, $\eta_c(f_s)$ is very small. Accordingly, if the f_- component is extracted as an output instead of the f_s component, then an efficient optical detection is possible. Therefore, Eq. (8) can be called the frequency conversion gain of the optical frequency conversion demodulation.

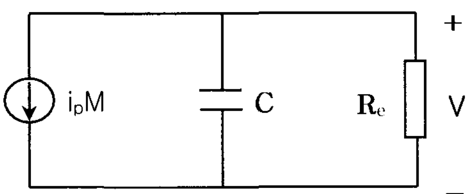

Fig. 3 Equivalent circuit of an APD

Table 2 APD parameters used in numerical calculation

Responsivity	0.85A/W
Breakdown voltage V_B	116V
Equivalent resistance R_{eq}	50Ω
Modulation index m	0.5
Materal index n	3
Input optical power P_o	20μW
Junction capacitance C_i	5pF
Cut-off frequency of APD (for C_i=5pF, R_{eq}=50Ω	2GHz

4. Numerical analysis by small signal model

Let us consider the equivalent circuit of the APD shown in Fig. 3. In this circuit, C is the sum of the internal and floating capacitance, and R_{eq} is the sum of the internal and external load resistance. The photo current $I_p(t)$ shown in Eq. (7) would be divided by the circuit admittance of $j\omega C$ and $1/R_{eq}$. Hence, the photo current of the sub-carrier frequency component f_s and down converted frequency component f_- are respectively

$$I(f_s) = M(V_b)\,|m|\,P_o\left(\frac{e}{h\nu}\right)\eta_p\left\{\frac{(1/R_{eq})^2}{\sqrt{(2\pi f_s C)^2+(1/R_{eq})^2}}\right\} \tag{9}$$

$$I(f_-) = \frac{1}{2}M'(V_b)V_l|m|P_o\left(\frac{e}{h\nu}\right)\eta_p\left\{\frac{(1/R_{eq})^2}{\sqrt{(2\pi f_- C)^2+(1/R_{eq})^2}}\right\} \tag{10}$$

Representing Eq. (8) in terms of Eq. (9) and (10),

$$G=\left|\frac{M'(V_b)V_l}{2M(V_b)}\right|\frac{\sqrt{(2\pi f_s C)^2+(1/R_{eq})^2}}{\sqrt{(2\pi f_- C)^2+(1/R_{eq})^2}} \tag{11}$$

In order to discuss the frequency conversion demodulation in detail, we carried out some calculations using the typical values as shown in Table 2. Fig. 4 shows the curves of the normalized gain, and the output power of the circuit versus the frequency difference f_- for some signal frequency f_s. Here, we assumed $V_b=116$V and $V_l=2$V . For simplicity, we chose the OMD to be 0.5. A larger gain is obtained for a higher signal frequency.

For example, the normalized gain is more than 6dB for $f_s=3$GHz, and about 2dB for $f_s=1$GHz. It is clear from Fig. 4(a) that the f_- component plays an important role in the mixing detection. This difference need to be smaller to make the gain larger. A zero frequency difference is desired to maximize the normalized gain. It is observed that the normalized gain is almost symmetrical with respect to the frequency difference. Fig. 4(b) shows the output power of the circuit. For direct detection, it is seen that the values of output power are unrelated to the frequency difference. However, they are related to the signal frequency. On the other hand, for mixing detection the values of output power are almost independent of the signal frequency. This indeed implies the feasibility of super-high-speed optical demodulation.

In Fig. 5, we present the curves of the normalized gain and the output power versus the signal frequency for some values of the frequency difference. The parameters for the calculation are the same as those in Fig. 4. From Fig. 5(a), we see again that for a fixed frequency difference, a larger gain can be obtained for a higher signal frequency and a lower frequency difference.

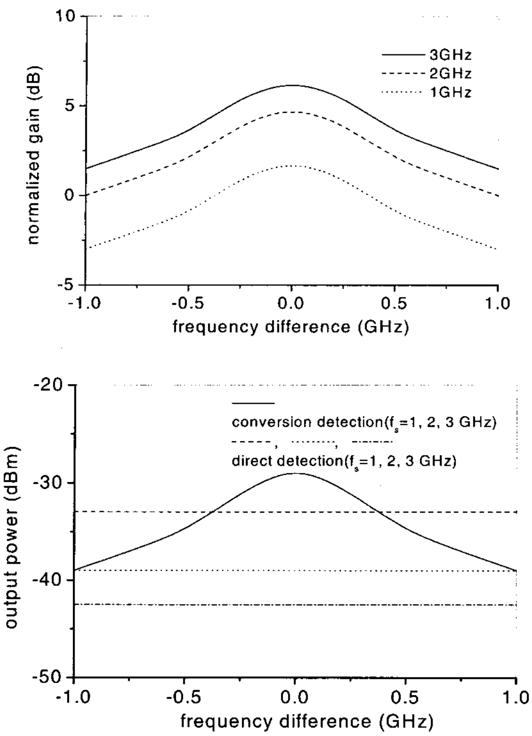

Fig. 4 Normalized gain output power vs. f_- frequency

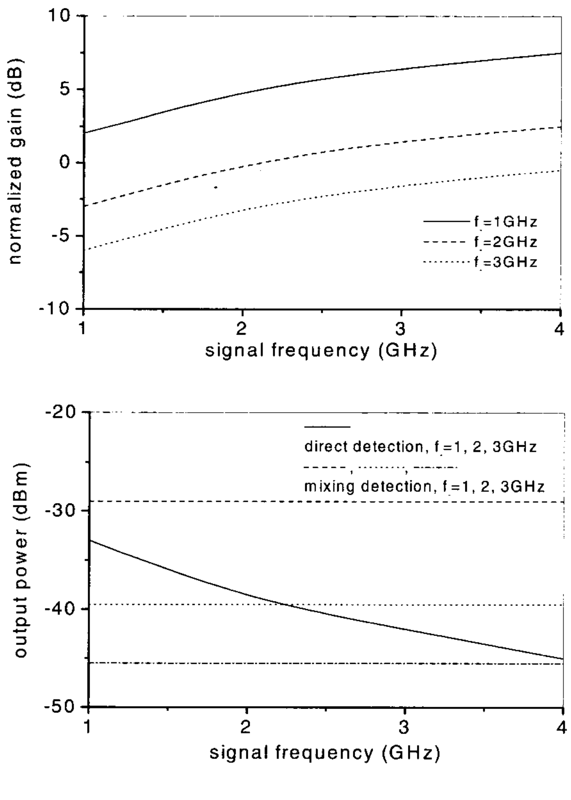

Fig. 5 Normalized gain and output power vs. signal frequency

It should be noted that since the signal frequency is determined by the transmitter, the only way to reduce the frequency difference in an actual application is to alter the local signal frequency. Fig. 5(b) shows the dependence of the output power on the signal frequency. It can be seen that when the signal frequency becomes higher, the power of direct detection will be less than that of down-converted detection. In practice, when the signal frequency becomes larger than the cut-off frequency of the APD, the signal power will drop rapidly. Thus, the actual gain of frequency conversion detecting may be much larger than that predicted by Fig. 4 and Fig. 5.

5. Experimental results

We have fabricated the demodulation circuit with an APD(Fu-04-AP-N by Mitsubishi) as shown in Fig. 2. A short wavelength laser(Fu-01-LD-N, wavelength 0.85μm) to be modulated directly was used as an optical source. The experimental setup was shown in Fig. 6. The modulated light wave is divided by an optical distributer,

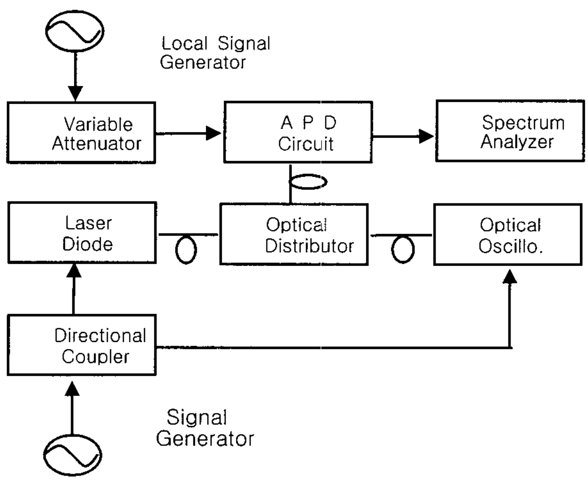

Fig. 6 Experimental setup

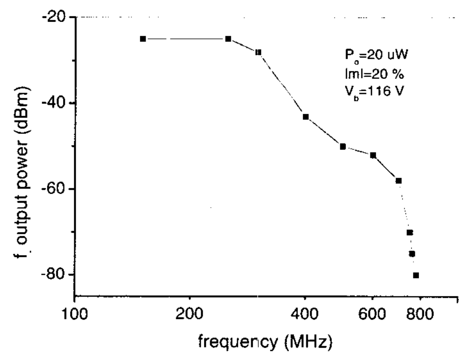

Fig. 7 Frequency characteristics of the demodulation circuit in which a 7pF capacitor is added in paralleled with the APD

and fed to the APD. The output of the APD was measured with a spectrum analyzer while the modulation index is monitored with an optical oscilloscope. Since it is expected that the efficiency of the frequency conversion demodulation differs in the regions above and below the cutoff frequency of the APD, we have separated these two cases.

Since the 3-dB cutoff frequency of the APD was 2GHz, the frequency conversion experiment was carried out for the light to be modulated at 1.3GHz which is below the directly detectable frequency of the APD. In this experiment, the bias voltage V_b of the APD was almost fixed at 116V. By applying the local signal of 1.26GHz, the different frequency output at 40MHz was measured. The relationship between the local signal input versus the difference frequency component output was shown in Fig. 7. When a local signal of more than 2dBm is applied, the output of the difference frequency component become larger than the directly detected output. Note that this difference component output increases linearly with the local signal input. Fig. 8 shows the frequency characteristics of the difference component output. As was expected in the theoretical analysis, the lower the difference frequency component is, the higher the output power was obtained.

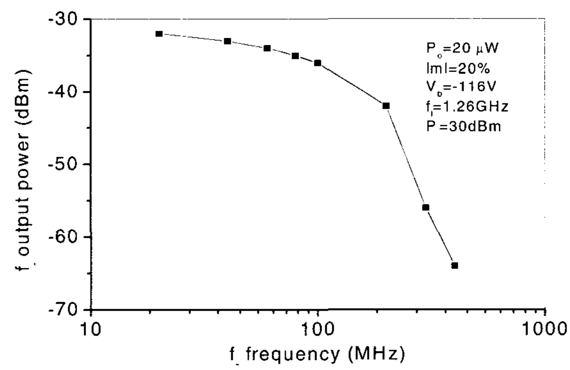

Fig. 8 Frequency characteristics of the f_- component output power

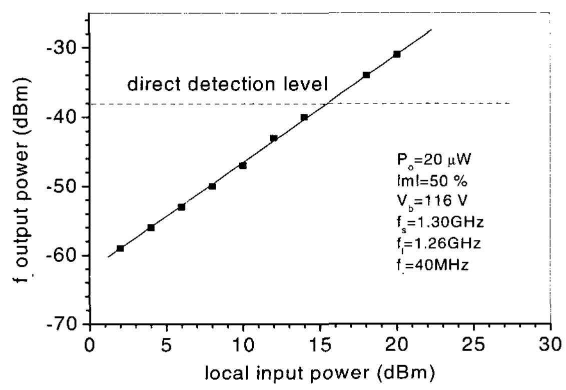

Fig. 9 f_- component output power at the frequency region below the cutoff frequency

Next, in order to carry out the demodulation experiment beyond the 3dB cutoff frequency region, a 7pF capacitor is added in parallel with the APD. The paralleled capacitor will reduce the frequency characteristics of the demodulation circuit. The frequency characteristics of the circuit are shown in Fig. 9. The results show that the directly detected outputs are negligible for frequencies over 700MHz. Since the directly detected signal is the smallest output at 780MHz, we applied the local signal of 1.26GHz, and a difference frequency output of 480MHz was observed. The results are shown in Fig. 10. For the local signal power of 1 0~20dBm, a difference component output of about 10dBm was obtained. The output also increases linearly with the local signal input.

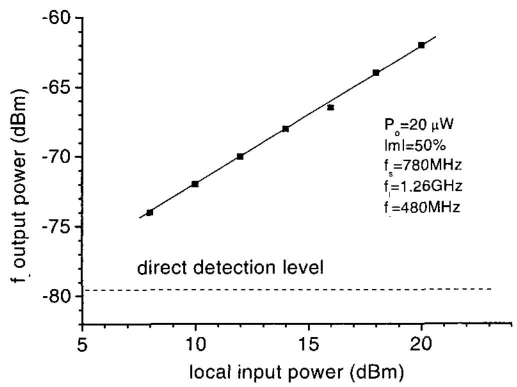

Fig. 10 f_- component output power at the frequency region beyond the cutoff frequency

6. Discussions

The above experimental results qualitatively agree with results of the fundamental analysis in Eq. (8). In the experiment of the frequency region below cutoff, the frequency conversion gain G exceeds 1 for the local signal input of more than 20dBm. It was also confirmed that η_c increases linearly as f_- becomes lower. In the case of the higher frequency region than the cutoff, $\eta_c(f_s)$ is more rapidly decreased. Hence, the ratio of $\eta_c(f_-)/\eta_c(f_s)$ increases so that the gain become larger than 1 even for the small local input power. It may be concluded that the higher the modulation frequency is, the larger the conversion efficiency is obtained.

In the experiments of a high frequency region above a detectable frequency, for many reasons combined with the experimental equipment of our Lab., 7pF capacitor was inserted on purpose in parallel with the APD so as to make the frequency characteristics of the APD poor. Accordingly, we need to carry out the experiments for a higher frequency region in the future.

7. Conclusions

We have extended the optical mixing detection theory to the undetectable frequency region of the APD. It was confirmed theoretically and experimentally that optical mixing detection is a more powerful technique in the undetectable frequency region of the photodiode. In the fundamental analysis, frequency characteristics of the multiplication factor of the APD, the frequency characteristics of η_p and the circuital efficiency of η_c are taken into consideration. We have used small signal analysis to investigate the frequency characteristics of an APD. A normalized gain has been introduced to analyze the performance of the mixing detection. The results can be summarized as follows. The difference frequency component is almost independent of the signal frequency, which implies that super-high-speed mixing demodulation is technically feasible for actual systems. The frequency difference between the original signal and the local signal should be as small as possible to achieve a large mixing output. And, the higher the signal frequency is, the larger the normalized gain can be obtained. The mixing detection of super-high-speed signals is attributed mainly to the nonlinearity of the multiplication factor. However, if a low dc bias voltage or a high ac local signal voltage is applied, the nonlinearity of the junction capacitance must be taken into consideration. It should be noted that the discussions of the study are based on the small signal analysis. There is an optimal local signal voltage (or an optimal dc bias voltage) in order to maximize the conversion gain. More detailed theoretical analysis and the experiments of a high frequency region will be carried out continuously in the future.

References

[1] D. G. Parker, P. G. Say, and W. Sibbett, "110GHz high-efficiency photodiodes fabricated from indium tin oxide/GaAs," Electron. Lett., vol. 23, no. 10, pp. 527-528, 1987.

[2] B. L. Kasper and J. C. Campbell, "Multibigabit-per-second avalanche photodiode lightwave receivers," IEEE J. Lightwave Technol. vol. LT-5, pp. 1351-1364, 1987.

[3] A. L. Peter, A. Andrekson, S. T. Eng, and A. Yariv, "Tunable super lattice p-i-n photodetectors : characteristics, theory, and applications," IEEE J. Quantum Electron., vol. 24, pp. 787-801, 1988.

[4] Alping A, "Waveguide pin photodetectors: theoretical analysis and design criteria", IEE Proc. 136, Pt. J. no. 3, pp. 177-182, June, 1989.

[5] T. Kagawa, K. Mogi, H. Iwamura, O. Mikami and M. Naganuma, "High speed low noise GaAs/AlGaAs superlattice APD", OQE89-22, May 1989.

[6] W. K. Kulczyk and Q. V. Davis "The avalanche photodiode as an electronic mixer in an optical receiver", IEEE Trans. Electron Devices, ED-19, 11, pp. 1181-1190, Nov. 1972.

[7] Q. V. Davis and W. K. Kulczk "Optical and electronic mixing in an avalanche photodiode", Electron Lett., 6. 2. Jan. 1980.

[8] A. J. Seeds and B. Lenoir, "Avalanche diode harmonic optoelectronic mixer", IEE Proc. Pt. J. 6. pp. 353-357, Dec. 1986.

[9] D. A. Humphreys, and R. A. Lobbett, "Investigation of an optoelectronic nonlinear effect in a GaInAs photodiode and its application in a coherent optical communication system", IEE Proc. 135, Pt. J. 1, Feb. 1988.

[10] S. M. Sze, "Physics of semiconductor devices", 2nd edition, John Wiley&Sons, 1981.

[11] H. F. Wolf, Handbook of fiber optics : theory and applications, Garland STPM Press, New York, 1979.

[12] T. E. Drace "Sub-carrier multiplexing for multiple-access lightwave networks", IEEE J. Lightwave Technol. LT-5, 8, pp. 1103-1110, 1987.

[13] T. E. Darcie et al. "Optical preamplifier for lightwave sub-carrier systems", Electron Lett. 25. 10, Feb. 1988.

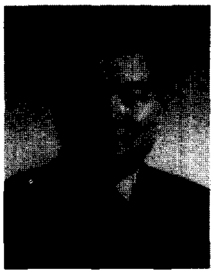

Young-Kyu Choi received his M. S. and Ph. D degrees from Kyoto University, Kyoto, Japan in 1989 and 1992, respectively. From 1993 to 1995, he was a full-time lecturer in the Department of El- ectronics, Fukui University, Fukui, Japan. He is now an associate professor of the Department of Photonics, Silla University, Busan, Korea. His research interests include the ultra-high-speed optical communication system, optical modulator and demodulator, optical waveguide analysis, optical sensors, microwave photonics, and near-field lightwave technology. He is presently a member of the KIEE, IEICE, JJAP, OSA, and IEEE.

Tel: +82-51-309-5622, Fax: +82-51-309-5622

E-mail: ykchoi@silla.ac.kr